J. Fluid Mech. (2011), *vol.* 684, *pp.* 163–191. © Cambridge University Press 2011
doi:10.1017/jfm.2011.288

Electrokinetics at liquid/liquid interfaces

Andrew J. Pascall and Todd M. Squires†

Department of Chemical Engineering, University of California, Santa Barbara, CA 93106, USA

(Received 30 January 2011; revised 28 May 2011; accepted 2 July 2011)

Electrokinetic effects at liquid/liquid interfaces have received considerably less attention than at solid/liquid interfaces. Because liquid/liquid interfaces are generally mobile, one might expect electrokinetic effects over a liquid/liquid interface to be faster than over an equivalent solid surface. The earliest predictions for the electrophoretic mobility of charged mercury drops – distinct approaches by Frumkin, along with Levich, and Booth – differed by $O(a/\lambda_D)$, where a is the radius of the drop and λ_D is the Debye length. Seeking to reconcile this rather striking discrepancy, Levine & O'Brien showed double-layer polarization to be the key ingredient. Without a physical mechanism by which electrokinetic effects are enhanced, however, it is difficult to know how general the enhancement is – whether it holds only for liquid metal surfaces, or more generally, for all liquid/liquid surfaces. By considering a series of systems in which a planar metal strip is coated with either a liquid metal or liquid dielectric, we show that the central physical mechanism behind the enhancement predicted by Frumkin is the presence of an unmatched electrical stress upon the electrolyte/liquid interface, which establishes a Marangoni stress on the droplet surface and drives it into motion. The source of the unbalanced electrokinetic stress on a liquid metal surface is clear – metals represent equipotential surfaces, so no field exists to drive an equal and opposite force on the surface charge. This might suggest that liquid metals represent a unique system, since dielectric liquids can support finite electric fields, which might be expected to exert an electrical stress on the surface charge that balances the electric stress. We demonstrate, however, that electrical and osmotic stresses on relaxed double layers internal to dielectric liquids precisely cancel, so that internal electrokinetic stresses generally vanish in closed, ideally polarizable liquids. The enhancement predicted by Frumkin for liquid mercury drops can thus be expected quite generally over ideally polarizable liquid drops. We then reconsider the electrophoretic mobility of spherical drops, and reconcile the approaches of Frumkin and Booth: Booth's neglect of double-layer polarization leads to a standard electro-osmotic flow, without the enhancement, and Frumkin's neglect of the detailed double-layer dynamics leads to the enhanced electrocapillary motion, but does not capture the (sub-dominant) electrophoretic motion. Finally, we show that, while the electrokinetic flow over electrodes coated with thin liquid films is $O(d/\lambda_D)$ faster than over solid/liquid interfaces, the Dukhin number, Du, which reflects the importance of surface conduction to bulk conduction, generally increases by a smaller amount $[O(d/L)]$, where d is the thickness of film and L is the length of the electrode. This suggests that liquid/liquid interfaces may be utilized to enhance

† Email address for correspondence: squires@engineering.ucsb.edu

https://doi.org/10.1017/jfm.2011.288 Published online by Cambridge University Press

electrokinetic velocities in microfluidic devices, while delaying the onset of high-*Du* electrokinetic suppression.

Key words: electrohydrodynamic effects, low-Reynolds-number flows, microfluidics

1. Introduction

Electrokinetic effects occur in systems wherein ions, electric fields, and surfaces interact to drive fluid and particulate motion. Their history is rich and venerable, dating back more than two centuries (Lyklema 2003). Electrokinetics continue to play a central role in colloid science (Russel, Saville & Schowalter 1989), analytical chemistry and molecular diagnostics (Landers 2003), genomic and proteomic separations (Görg, Weiss & Dunn 2004; Dorfman 2010), micro- and nanofluidics (Squires & Quake 2005; Schoch, Han & Renaud 2008; Bocquet & Charlaix 2010), and directed colloidal assembly (Velev & Bhatt 2006).

A recent development that has revealed qualitatively new electrokinetic behaviour involves the no-slip boundary condition, which is now known to fail in certain solid/fluid systems (Lauga, Brenner & Stone 2007; Bocquet & Charlaix 2010), particularly at hydrophobic solid/liquid interfaces. The simplest generalization to account for solid/liquid slip is the Navier slip condition,

$$u_s(y=0) = \beta \left.\frac{\partial u}{\partial y}\right|_{y=0}, \tag{1.1}$$

where β is the so-called slip length, u_s is the fluid velocity parallel to the solid surface located at $y = 0$, and y is the coordinate perpendicular to the surface. Finite slip lengths can naturally enhance electro-osmotic flow velocities quite significantly (Muller *et al.* 1986; Churaev *et al.* 2002; Joly *et al.* 2006; Bouzigues, Tabeling & Bocquet 2008; Tandon & Kirby 2008; Squires 2008; Khair & Squires 2009*a*; Audry *et al.* 2010; Bahga, Vinogradova & Bazant 2010; Bocquet & Charlaix 2010), giving an enhancement

$$U^S = U^{EOF}\left(1 + \frac{\beta}{\lambda_D}\right). \tag{1.2}$$

The reason is clear: electrokinetic shear rates inside the double layer scale like $\dot{\gamma} = U^{EOF}/\lambda_D$, where λ_D is the Debye screening length, which give rise to an interfacial slip velocity that is larger than U^{EOF} by a factor β/λ_D. Since λ_D is often small (O(nm)), the slip length β need not be very large before the enhancement becomes significant or even dominant. This formula holds only for homogeneously slipping surfaces; heterogeneities in either slip length or charge profiles give rise to significantly modified formulae (Squires 2008; Bahga *et al.* 2010). Furthermore, Khair & Squires (2009*a*) showed slip to similarly enhance the electroconvective component of the surface conduction, and thus hasten the high-*Du* suppression of electrokinetic effects. Here *Du* is the Dukhin number, which reflects the importance of surface conduction to bulk conduction, as discussed in § 8. Nonetheless, for uniformly slipping surfaces, Bouzigues *et al.* (2008) provide experimental measurements of the slip length using pressure/flow rate measurements, hindered diffusivity, and electrokinetic flows that yield consistent results for the slip length for all three independent measurement

https://doi.org/10.1017/jfm.2011.288 Published online by Cambridge University Press

techniques. Pennathur, Eijkel & van den Berg (2007), Davidson & Xuan (2008) and Ren & Stein (2008) argue that such slip could significantly enhance the efficiency of electrokinetic energy conversion using nanochannels.

While the vast majority of studies of electrokinetic effects have concerned solid/liquid interfaces, with relatively little attention paid to liquid/liquid interfaces, liquid/liquid interfaces provide a different means of achieving effective slip at electrolyte boundaries. A shear stress, τ, applied along a clean liquid/liquid film of thickness d_f and viscosity η drives a flow within the film with an interfacial velocity

$$U_{int} \sim \frac{d_f \tau}{\eta} \sim d_f \frac{\partial u_f}{\partial y}, \tag{1.3}$$

which bears similarity to the Navier slip condition (1.1). Engineering thin liquid films, then, may provide stable, robust and tunable ways to give large effective slip in electrokinetic systems, and may alleviate the flow suppression at high Du, as discussed in § 8.

2. Background

The first rigorous attempt to solve for the electrophoretic motion of liquid drops was made by Booth (1951), who adapted a theory put forth by Henry (1931) to account for a liquid/liquid boundary. Booth obtained

$$\boldsymbol{U} = \frac{6\eta_i(1+\lambda) + 4\eta_e(1-2\lambda)}{(9\eta_i + 6\eta_e)} \frac{\varepsilon_e \zeta \boldsymbol{E}}{\eta_e}, \tag{2.1}$$

for the translational velocity of the drop, where

$$\lambda = \frac{\sigma_e - \sigma_i}{2\sigma_e + \sigma_i}. \tag{2.2}$$

Here, the subscripts 'e' and 'i' represent the properties of the electrolyte and drop, respectively; η, ε, and σ are the viscosity, electric permittivity and conductivity. The potential drop across the double layer external to the drop is ζ and $\boldsymbol{E}$ is the applied electric field. Notably, Booth (1951) followed the prevailing approach for electrokinetics, which expressly accounted for the forces exerted on the fluid within an explicitly computed double layer. Booth, like Henry (1931), assumed that the double layer remained unperturbed under the applied electric field and that an electrical current could flow through the interface.

Frumkin (1946), along with Levich, put forth a theory for the electrophoresis of liquid mercury drops, in which they followed a completely different approach (see Levich 1962 for a more accessible description). Rather than explicitly resolving the forces within the double layer, Frumkin (1946) argued that the double layer around an ideally polarizable object will, by nature, be polarized, giving a zeta potential that varies along the interface. An electrostatic potential drop across an interface modifies the interfacial tension, γ, via the Lippmann–Helmholtz equation,

$$\gamma(V) = \gamma_{eq} - \frac{qV}{2}, \tag{2.3}$$

where q is the charge per unit area on the interface and V is the potential drop across the interface. Frumkin and Levich argued that gradients in zeta potential along the interface give rise to surface tension gradients, which, in turn, drive Marangoni flows and thus electrocapillary motion. The surface tension gradients scale like $\nabla\gamma \sim q\nabla V$.

https://doi.org/10.1017/jfm.2011.288 Published online by Cambridge University Press

Since $\nabla V \sim \boldsymbol{E}$ and $q \sim \varepsilon\zeta/\lambda_D$ in the low-ζ limit, a Marangoni stress is exerted upon the interface

$$\tau \sim \frac{\varepsilon\zeta E}{\lambda_D}, \tag{2.4}$$

which drives the flow. Frumkin (1946) solved for the Stokes flows inside and outside the drop, subject to a no-slip condition $u_e(r=a) = u_d(r=a)$ and a tangential stress jump given by (2.4), to arrive at the electrophoretic mobility of a liquid metal drop,

$$U = \frac{\varepsilon_e \zeta E a}{\lambda_D(3\eta_i + 2\eta_e)}. \tag{2.5}$$

Notably, the Frumkin–Levich scaling (2.5) significantly exceeds the Booth mobility (2.1), by a factor a/λ_D, with $\lambda \to -1$ since $\sigma_d \gg \sigma_e$ for mercury drops. The scaling can be understood in a straightforward fashion: the tangential stress jump (2.4) is balanced by viscous stresses $\tau \sim \eta U_0/a$, whose gradient length scale is set by the droplet radius a, to give a velocity scale $U_0 \sim (\varepsilon\zeta E/\eta)a/\lambda_D$. Bagotskaya (1949)'s experimental study of the electrophoresis of mercury drops (summarized in English by Levich 1962) is consistent with the theoretical predictions of Frumkin and Levich, while additional experimental work on the movement of mercury drops in electric fields has focused on regimes outside those originally considered by Frumkin and Levich or by Booth (Poigin *et al.* 1977; Gorre, Ioannidis & Silberzan 1996; Gorre-Talini & Silberzan 1997).

Levine & O'Brien (1973) sought to reconcile this rather striking discrepancy between Booth and Frumkin. They argued that the crucial difference between the starting assumptions involved Booth's neglect of double-layer polarization arising from the applied electric field. Indeed, they found that explicitly neglecting polarization gave results consistent with Booth (1951), whereas including double-layer polarization gave mobilities consistent with Frumkin (1946). Ohshima, Healy & White (1984) then adapted the numerical scheme of O'Brien & White (1978) for electrophoresis to allow for liquid mercury drops and demonstrated that the enhanced formula holds only for very low ζ. This result will be discussed in greater detail in § 8.

Although Levine & O'Brien identified double-layer polarization as a necessary component for the enhanced electrophoretic mobilities of liquid drops, the mechanism behind its operation remains unclear. How exactly does polarization give rise to the enhancement, and when can such enhanced flows be expected more generally? Questions of fundamental and applied importance persist. For example, electro-osmotic flows are deliberately engineered in microfluidic systems, particularly induced-charge electrokinetic systems (Squires & Bazant 2004; Bazant & Squires 2010). Can their magnitude be enhanced using thin liquid films? If so, does the enhancement only occur for liquid metal surfaces, or does it occur more generally with liquids of finite or low conductivity? In fact, the liquid metal may itself present a singular limit, in which the enhancement occurs because the surface charge density is located where the electric field is defined to be zero. If one considers a highly (but not infinitely) conductive liquid, with an (internal) surface charge density of finite thickness λ_{Di}, which can support a non-zero elecric field within λ_{Di}, does one recover the liquid metal result in the limit $\lambda_{Di} \to 0$, or does that result only hold for $\lambda_{Di} = 0$? In other words, can this enhancement be expected more generally over liquid/liquid interfaces?

Here we address these questions, clearly elucidating the physical mechanism behind Levich and Frumkin's electrokinetic enhancement. In § 3, we begin by studying the electrokinetic flow over a solid planar metal strip in the limit where the double layer

https://doi.org/10.1017/jfm.2011.288 Published online by Cambridge University Press

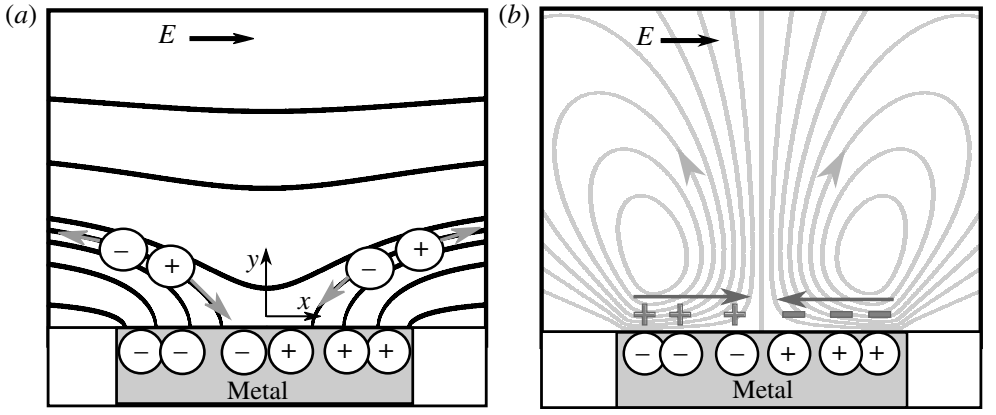


FIGURE 1. Induced-charge electro-osmosis (ICEO) over an ideally polarizable planar strip. (*a*) Immediately after an electric field, E, is applied, the metal strip polarizes and electric field (black lines) intersect the metal surface at right angles. Ions from the bulk electrolyte are forced along field lines to screen the surface charge. (*b*) Steady state is reached when just enough charge is forced into the induced double layer to exactly compensate the polarized surface charge on the metal strip. An electro-osmotic flow (grey lines) results from the interaction of the charged double layer and the applied field. Note: only the flow due to ICEO is represented in the figure.

is much thinner than the width of the strip. We move to an analysis of the flow over a liquid metal strip in § 4 and demonstrate that it is the lack of an equal and opposite electrical stress at the electrolyte/metal interface (due to the lack of a field within the metal) that leads to the velocity enhancement. In § 5, we show that the enhancement occurs for moderately conductive liquids as well. More generally, we show that the total electrokinetic stress on a double layer inside any ideally polarizable interface is zero at steady state, leading to unbalanced electrical stresses in liquid/liquid systems. In § 6, we show that the non-zero interfacial electrical stress jump results directly from the double layer being in quasi-equilibrium with the adjacent bulk and derive the general result in terms of an electrochemical potential. We revisit the electrophoresis of a liquid metal drop under the newly developed framework in § 7 and find that Frumkin and Levich's electrocapillary approach provides the correct mobility to leading order, but neglects the subdominant contribution of electro-osmosis to the mobility. In § 8, we discuss the effects of surface conduction and interface 'solidification' as defined by Ohshima *et al.* (1984). Finally, in § 9, we offer concluding remarks and discuss various experimental systems that may be useful for observing the effects described herein.

3. Electro-osmotic flow over a solid metal strip

We will begin by examining a related, but geometrically simpler problem: electro-osmotic flow over an ideally polarizable, solid metal strip (figure 1). This is the geometry studied by Mansuripur, Pascall & Squires (2009) and Pascall & Squires (2010*a*,*b*). For simplicity, we consider a 1:1 symmetric electrolyte with an electric field, $\boldsymbol{E} = E_0\hat{\boldsymbol{x}}$, applied to the bulk. Throughout this work, we will assume the external double layer to be much thinner than the length of the electrode, $\lambda_D \ll L$, and our analysis will only be valid far from the electrode edges. Our analysis will mirror that of Squires & Bazant (2004): we will first the derive the electrostatic potential in the

https://doi.org/10.1017/jfm.2011.288 Published online by Cambridge University Press

electrolyte, then the electrostatic and osmotic body force exerted on the fluid within the double layer, and finally, we solve for the electro-osmotic 'slip' velocity outside the double layer.

The total electrostatic potential, ϕ, is the superposition of the potential due to the applied field, ϕ_{app}, and the potential due to ions in the double layer near the surface, ϕ_{DL},

$$\phi = \phi_{app} + \phi_{DL}, \tag{3.1}$$

and obeys boundary conditions:

$$\phi(y \to \infty) \to -Ex, \tag{3.2a}$$

$$\phi(y = 0) = \zeta_0, \tag{3.2b}$$

where ζ_0 is the native equilibrium surface potential. For simplicity, we will assume that the native surface potential of the electrode, ζ_0, and the applied potential, $E_0 x$, are, in total, much smaller than the thermal voltage, $\zeta_0 + E_0 x \ll k_B T/e$.

Since the bulk electrolyte is electroneutral, the applied potential obeys Laplace's equation:

$$\nabla^2 \phi_{app} = 0. \tag{3.3}$$

Immediately after the potential is applied, the metal strip polarizes and electric field lines intersect the metal surface at right angles. A current flows into the double layer from the bulk (figure 1*a*). The ideal polarizability of the metal surface precludes any current from flowing across the electrolyte/metal interface, so the current builds an induced double layer that screens the polarized metal strip. Steady state is reached when the current injects just enough charge into the induced double layer to exactly compensate for the polarized surface charge on the metal strip (figure 1*b*). At steady state, the normal component of the electric field vanishes, so that the applied potential ϕ_{app} obeys a no-flux (insulating) boundary condition at the edge of the double layer:

$$\left.\frac{\mathrm{d}\phi_{app}}{\mathrm{d}y}\right|_{y=0} = 0. \tag{3.4}$$

This boundary condition generally holds at ideally polarizable surfaces, in steady state, whenever surface conductivity (parameterized by the dimensionless Dukhin number, Du) is negligible. Strongly charged surfaces with finite Du require an ion flux to and from the electroneutral bulk, modifying both the tangential field and introducing bulk concentration gradients (Lyklema 1995; Khair & Squires 2009*a*). Throughout this work, we assume that the $Du \to 0$ limit of negligible surface conduction holds, but non-zero Dukhin number effects at liquid/liquid interfaces will be discussed in § 8. In the $Du \to 0$ limit, the applied potential is given by

$$\phi_{app} = -E_0 x. \tag{3.5}$$

The electrostatic potential within the double layer, ϕ_{DL}, obeys the Poisson–Boltzmann equation,

$$\nabla^2 \phi_{DL} = \lambda_D^{-2} \phi_{DL}, \tag{3.6}$$

which has been linearized under the simplifying assumption of low zeta potentials. The boundary condition on the total potential at the surface (3.2*b*) requires that

$$\phi_{DL}(y = 0) = \zeta_0 + E_0 x, \tag{3.7}$$

https://doi.org/10.1017/jfm.2011.288 Published online by Cambridge University Press

while in the far field, the double-layer potential must vanish. In the limit of thin double layer, the double-layer potential is thus given by

$$\phi_{DL} = (\zeta_0 + E_0 x)\mathrm{e}^{-y/\lambda_D}. \tag{3.8}$$

From (3.5) and (3.8), the total potential in the electrolyte is, therefore,

$$\phi(x, y) = \zeta(x)\mathrm{e}^{-y/\lambda_D} - E_0 x, \tag{3.9}$$

where, for convenience, the total zeta potential,

$$\zeta(x) \equiv \zeta_0 + E_0 x, \tag{3.10}$$

has been defined as the sum of the native and induced zeta potentials.

Having solved for the electrostatic field, we now turn to the electrokinetic flow. The tangential electric field,

$$-\nabla_{\parallel}\phi = E_0[1 - \mathrm{e}^{-y/\lambda_D}], \tag{3.11}$$

drives the free charge density within the double layer,

$$\rho = -\varepsilon_e \nabla^2 \phi_{DL} = -\frac{\varepsilon_e}{\lambda_D^2}\zeta(x)\mathrm{e}^{-y/\lambda_D}, \tag{3.12}$$

to exert a body force

$$\boldsymbol{f}_{ele} = \rho \boldsymbol{E} \tag{3.13a}$$

$$= -\frac{\varepsilon_e}{\lambda_D^2}\zeta(x)E_0[\mathrm{e}^{-y/\lambda_D} - \mathrm{e}^{-2y/\lambda_D}] \tag{3.13b}$$

on the fluid which drives an electro-osmotic flow. Notably, the electric field vanishes at the metal surface ($y = 0$), in contrast to standard electro-osmotic flow.

In addition to the electrical body force (3.13*a*), each ion is driven by an osmotic force

$$\boldsymbol{F}_{osm}^{\pm} = -k_B T \nabla \log n_{\pm}, \tag{3.14}$$

giving a total osmotic body force density

$$\boldsymbol{f}_{osm} \equiv \sum n_{\pm} \boldsymbol{F}_{osm}^{\pm} = -k_B T \nabla (n_+ + n_-) \tag{3.15}$$

which arises from gradients within the polarized double layer.

Levich (1962) showed that these two body forces combine to take a particularly simple form, $\rho(x)E_0$, involving the local charge density and the electric field in the bulk. This can be seen by considering the gradients in ion concentration along the interface. Since the ions follow the Boltzmann distribution, the concentration of ions in the double layer for a 1:1 electrolyte is

$$n_+ + n_- = 2n_0 \cosh\left(\frac{e\phi_{DL}}{k_B T}\right). \tag{3.16}$$

The osmotic body force (3.15) thus becomes

$$\boldsymbol{f}_{osm} = -2n_0 e \sinh\left(\frac{e\phi_{DL}}{k_B T}\right)\nabla\phi_{DL} \equiv \rho \nabla \phi_{DL}, \tag{3.17}$$

since

$$\rho = e(n_+ - n_-) = -2en_0 \sinh\left(\frac{e\phi_{DL}}{k_B T}\right). \tag{3.18}$$

https://doi.org/10.1017/jfm.2011.288 Published online by Cambridge University Press

The total body force on a fluid element in the double layer is the sum of (3.13*a*) and (3.17),

$$\boldsymbol{f} = \boldsymbol{f}_{ele} + \boldsymbol{f}_{osm} = -\rho(\nabla\phi_{app} + \nabla\phi_{DL}) + \rho\nabla\phi_{DL} \equiv -\rho\nabla\phi_{app}, \tag{3.19}$$

and reduces simply to the product of the free charge density with the applied electric field (Levich 1962; Squires & Bazant 2004) (figure 3*c*).

The Reynolds numbers of electrokinetic flows are typically small ($Re \ll 1$) as the characteristic dimensions are usually O (μm), while flow rates are generally no greater than O (mm s^{-1}). Furthermore, only quasi-steady flows are considered here, so the fluid flow is described by the incompressible, steady Stokes equations, with electrical and osmotic body forces:

$$\eta_e\nabla^2\boldsymbol{u} - \nabla P + \boldsymbol{f} = 0, \tag{3.20a}$$

$$\nabla\cdot\boldsymbol{u} = 0. \tag{3.20b}$$

Inspection of the form of ϕ (3.9) shows that gradients normal to the surface occur over a length scale, λ_D, which is much smaller than the length scale of gradients tangent to the surface, L. Therefore, we follow a lubrication-style approximation, which neglects velocity gradients tangent to the surface, to give a general solution for the velocity field tangent to the surface:

$$u_x(x, y) = A + By + Cy^2 + \frac{\varepsilon_e\zeta(x)E_0}{\eta_e}\mathrm{e}^{-y/\lambda_D}, \tag{3.21}$$

where a uniform pressure gradient ($-C$) has been assumed. The no-slip condition at the electrolyte/solid interface ($y = 0$) requires that

$$A = -\frac{\varepsilon_e\zeta(x)E_0}{\eta_e}. \tag{3.22}$$

The bulk is electroneutral and concentration gradients are confined to the double layer; therefore, there is no stress in the bulk. This implies

$$\left.\frac{\mathrm{d}u}{\mathrm{d}y}\right|_{y\to\infty} = 0, \tag{3.23}$$

so

$$B = C = 0. \tag{3.24}$$

Thus, the flow tangent to the metal surface is

$$u_x(x, y) = -\frac{\varepsilon_e\zeta(x)E_0}{\eta_e}[1 - \mathrm{e}^{-y/\lambda_D}]. \tag{3.25}$$

The bulk electrolyte is thus driven by an electrokinetic 'slip' velocity, just outside the double layer, given by

$$u_s = -\frac{\varepsilon_e(\zeta_0 + E_0x)E_0}{\eta_e}. \tag{3.26}$$

This represents the quasi-steady ICEO slip velocity over the planar metallic strip geometry that was examined theoretically and experimentally by Mansuripur *et al.* (2009) and Pascall & Squires (2010*a*,*b*). It is entirely analogous to the ICEO slip flows described by Gamayunov, Mantrov & Murtsovkin (1992), Murtsovkin (1996)

https://doi.org/10.1017/jfm.2011.288 Published online by Cambridge University Press

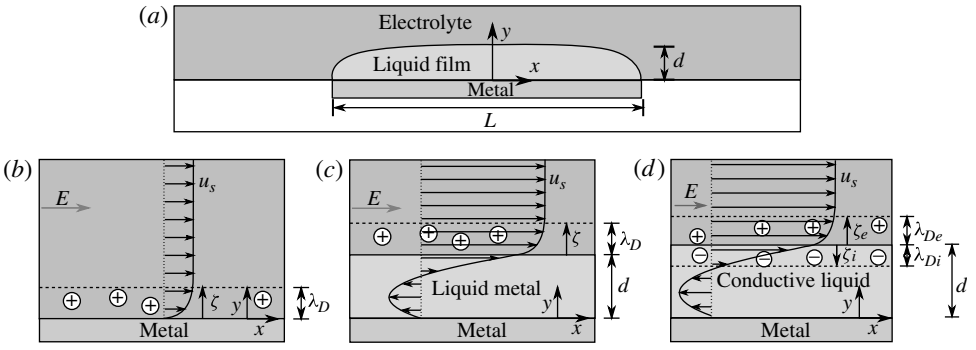


FIGURE 2. (*a*) A thin liquid film of thickness d is placed on a metal strip of width L. (*b*) When the thin film is not present, the no-slip condition requires that the electro-osmotic flow velocity vanish at the metal surface. The stresses exerted by the double layer on the interface are balanced by minute elastic deformations of the metal. (*c*) When a liquid metal is used as a thin film, the electric field at the liquid/liquid interface must vanish. The electrical stress in the double layer can only be balanced by viscous stresses in the film, leading to an enhanced slip velocity. (*d*) The electric field can penetrate into a conductive dielectric liquid, which leads to the formation of double layers on both sides of the interface. However, the net electrokinetic stress is zero on the internal double layer. Again, the electric stress in the external double layer can only be balanced by viscous stresses in the film, leading to a similar slip velocity enhancement.

and Squires & Bazant (2004) for cylinders and spheres, and represents the classical Helmholtz–Smoluchowski formula modified to account for induced charge effects.

This investigation of the electro-osmotic flow (both fixed-charge and induced-charge) over a solid metal planar strip will serve as a standard against which to examine electro-osmotic flows over liquid/liquid interfaces. An important feature is that the polarization of the double layer gives rise to osmotic pressure gradients (3.17) of the same order as the electrical forces on the double layer. Additionally, the no-slip condition at the solid/liquid interface requires the velocity to be zero at the interface itself. This results in a classical electro-osmotic slip, where velocity gradients are confined to the double layer. The electro-osmotic slip velocity (3.26) thus arises as a 'velocity jump' across the double layer, independent of the double-layer thickness.

We will now treat a closely related problem in which a thin liquid metal layer coats the solid metal strip, and shall see how and why the effective electro-osmotic slip is enhanced.

4. Electro-osmotic flow over a liquid metal thin film

We now examine the effects of a liquid/liquid interface by considering the solid metal strip studied in the previous section to be coated with a liquid metal film of viscosity η_i and thickness d, such that $\lambda_D \ll d \ll L$ (figure 2*c*). We will proceed as before and begin by discussing the electrostatics in the electrolyte and the liquid metal film. Then, we will consider the flow profile in both the electrolyte and liquid film far from the electrode edges under the same assumptions as in § 3.

The electrostatic potential follows directly from § 3, as both the applied and double-layer potentials satisfy the same equations (3.3) and (3.6), subject to the same boundary conditions (3.2*a*) and (3.2*b*), with the only difference being that the liquid/liquid interface is located at $y = d$. The total potential in the electrolyte is thus

https://doi.org/10.1017/jfm.2011.288 Published online by Cambridge University Press

given by

$$\phi_e(x, y) = \zeta(x)\mathrm{e}^{-(y-d)/\lambda_D} - E_0 x, \tag{4.1}$$

where $\zeta(x)$ is given by (3.10). Since the interior of the liquid metal cannot support an electric field, its electrostatic potential is constant everywhere: $\phi_m = \zeta_0$.

The fluid flow in both the electrolyte and metal are governed by the incompressible forced Stokes equations (3.20). As above, the body force on the double layer arises due to both the space charge in the double layer as well as the osmotic pressure gradient along the polarized double layer, which combine to a form $f = \rho(x)E_0$. Since the electric field vanishes in the liquid metal and on its surface, the liquid metal experiences no body force or electrical stress at $y = d$. The general solutions for the flow in the electrolyte, u_e, and the film, u_f, are given by

$$u_e(x, y) = A + By + Cy^2 + \frac{\varepsilon_e \zeta(x) E_0}{\eta_e}\mathrm{e}^{-(y-d)/\lambda_D}, \tag{4.2a}$$

$$u_f(x, y) = D + Ey + Fy^2, \tag{4.2b}$$

where the constants A–F are determined to satisfy boundary conditions.

The no-stress condition in the bulk electrolyte (3.23) requires that $B = C = 0$, while the no-slip condition at the solid/liquid interface requires $D = 0$. The flow in the film is coupled to the flow in the electrolyte by the interfacial boundary conditions of no-slip and continuity of shear stress:

$$u_e(x, d) = u_f(x, d), \tag{4.3a}$$

$$\eta_e \left.\frac{\partial u_e}{\partial y}\right|_{y=d} = \eta_i \left.\frac{\partial u_f}{\partial y}\right|_{y=d}. \tag{4.3b}$$

The final constraint is the conservation of mass in the film:

$$\int_0^d u_m \,\mathrm{d}y = 0. \tag{4.4}$$

All remaining integration constants in (4.2) can now be determined, yielding

$$u_e(x, y) = -\frac{\varepsilon_e}{\eta_e}\zeta(x)E_0\left(1 + \frac{1}{4}\frac{\eta_e}{\eta_i}\frac{d}{\lambda_D}\right) + \frac{\varepsilon_e \zeta(x) E_0}{\eta_e}\mathrm{e}^{-(y-d)/\lambda_D}, \tag{4.5a}$$

$$u_f(x, y) = \frac{1}{2}\frac{\varepsilon_e}{\eta_i}\zeta(x)E_0\left(\frac{y}{\lambda_D} - \frac{3}{2}\frac{y^2}{\lambda_D d}\right). \tag{4.5b}$$

The slip velocity over a liquid metal surface [$u_e(x, y - d \gg \lambda_D)$] is enhanced relative to the flow over the analogous solid metal strip (3.26):

$$\frac{u_{sLM}}{u_s} = \left(1 + \frac{1}{4}\frac{\eta_e}{\eta_i}\frac{d}{\lambda_D}\right). \tag{4.6}$$

This enhancement occurs because the electrolyte/liquid metal interface itself moves with velocity

$$U_i = u_e(x, d) = u_f(x, d) = -\frac{\varepsilon_e}{\eta_e}\zeta(x)E_0\left(\frac{1}{4}\frac{\eta_e}{\eta_i}\frac{d}{\lambda_D}\right), \tag{4.7}$$

in response to the tangential electrical stress exerted within the double layer and the lack of an equal and opposite electrical stress within the liquid metal. A solid metal

https://doi.org/10.1017/jfm.2011.288 Published online by Cambridge University Press

surface (as in § 3) is also subjected to this large electrical stress, but balances this stress with small elastic deformations. A liquid metal surface, on the other hand, subjected to an imposed shear stress, is driven to flow at a velocity that establishes a viscous stress sufficient to balance the imposed electrical stress. The relation given in (4.6) suggests a straightforward method for verifying the theory derived above: the observed slip velocity over a liquid metal thin film should increase linearly with increasing film thickness.

Frumkin (1946) used the Lippmann–Helmholtz equation (2.3) to relate the surface tension at the electrolyte/liquid metal interface to the local zeta potential. Doing so for the present geometry gives

$$\gamma(x) = \gamma_{eq} - \frac{q\zeta(x)}{2} = \gamma_{eq} + \frac{\varepsilon_e \zeta(x)^2}{2\lambda_D}, \tag{4.8}$$

where the surface charge density, $q \equiv -\int_d^\infty \rho \, \mathrm{d}y$. The zeta potential variation along the metal surface thus gives rise to a Marangoni stress,

$$\tau(x) = \frac{\partial \gamma}{\partial x} = \frac{\varepsilon_e}{\lambda_D}\zeta(x)E_0, \tag{4.9}$$

at the interface (figure 3*b*). Solving the thin film problem subject to this Marangoni stress (4.9) at $y = d$ gives (4.5*b*), revealing the velocity of the liquid/liquid interface itself to be

$$U = \frac{1}{4}\frac{\varepsilon_e \zeta(x) E_o}{\eta_i}\frac{d}{\lambda_D}, \tag{4.10}$$

which matches (4.6) to leading order. Frumkin and Levich's argument is based on the thermodynamics of the interface and neglects all details within the liquid metal/double-layer interface. Therefore, it cannot capture the (subdominant) electro-osmotic velocity jump across the double layer. By examining the stress distribution within the liquid metal/double-layer interface, both the (dominant) electrocapillary term of Levich (1962) and the subdominant electro-osmotic velocity are recovered in (4.6).

We have shown that the electrokinetic velocity enhancement at electrolyte/liquid metal interfaces is caused by an unbalanced electrical stress applied along the interface. In this case, the lack of an equal and opposite electrical stress within the liquid metal – due to the equipotential nature of metals – is clearly responsible.

At this point, however, it remains unclear whether such enhancements are unique to liquid metal surfaces, or whether they occur more generally in liquid/liquid systems, which can support non-zero electric fields. In the next section, the assumption of infinite conductivity of the thin film is relaxed, and we study the flow over a metal strip coated with a thin film of a moderately conductive liquid. We show that, in fact, this electrical stress imbalance occurs generally around ideally polarizable interfaces between conductive liquids.

5. Electro-osmotic flow over a conductive dielectric liquid thin film

In this section, we relax the assumption of infinite electrical conductivity of the thin film and consider the electro-osmotic flow over a thin film of a dielectric liquid of permittivity ε_i, conductivity σ_i, and thickness d atop a metal strip of length L (figure 2*d*). We will assume that both the liquid/liquid and liquid/metal interfaces are ideally polarizable, and, initially, that the double layer thicknesses are thinner than any

https://doi.org/10.1017/jfm.2011.288 Published online by Cambridge University Press

geometric length scale ($\lambda_{De}, \lambda_{Di} \ll d \ll L$). Later, we will relax the assumption of a thin internal double layer and compute the solution for an arbitrarily thick equilibrium internal double layer. We will follow the same procedure as in the previous sections: first, we compute the electrostatic potential in both the electrolyte and thin film; then find the electrokinetic body force exerted on the double layers; and, ultimately, compute the flow profile in the electrolyte and film from the forced Stokes equations.

The electric field applied in the bulk electrolyte is coupled to the electric field in the thin film through the liquid/liquid interface. In response to the field, two back-to-back double layers form at the interface such that the applied potential in the bulk electrolyte,

$$\phi_{app_e} = -E_0 x, \tag{5.1}$$

is dropped across both double layers (figure 2*d*). In order to determine how the total potential drop is partitioned between the two double layers, we will again consider the total electrostatic potential in each phase to be composed of a potential due to the charge in each double layer, which obeys the Poisson–Boltzmann equation (3.6) and the applied potential. At steady state, no current can flow within the thin film. Thus, the applied potential in the internal phase, ϕ_{app_i}, must be constant, which here is set to give zero induced charge at the midplane of the film.

The total potential in each phase can be written generally as

$$\phi_e(x, y) = A\mathrm{e}^{-(y-d)/\lambda_{De}} + B\mathrm{e}^{(y-d)/\lambda_{De}} - E_0 x, \tag{5.2a}$$

$$\phi_i(x, y) = C\mathrm{e}^{-(y-d)/\lambda_{Di}} + D\mathrm{e}^{(y-d)/\lambda_{Di}}, \tag{5.2b}$$

where the constants A–D are determined by boundary conditions. The far-field boundary condition requires that

$$\phi_{e,i} \to \phi_{app_{e,i}}, \tag{5.3}$$

which forces $B = C = 0$. At the interface, the electrostatic potential and the displacement electric field must be continuous:

$$\phi_e(x, d) = \phi_i(x, d), \tag{5.4a}$$

$$\varepsilon_e \left.\frac{\partial \phi_e}{\partial y}\right|_{y=d} = \varepsilon_i \left.\frac{\partial \phi_i}{\partial y}\right|_{y=d}. \tag{5.4b}$$

This leads to a total potential in each phase near the interface of

$$\phi_e(x, y) = \left(\frac{E_0 x}{1+\delta}\right)\mathrm{e}^{-(y-d)/\lambda_{De}} - E_0 x, \tag{5.5a}$$

$$\phi_i(x, y) = -\left(\frac{\delta E_0 x}{1+\delta}\right)\mathrm{e}^{(y-d)/\lambda_{Di}}, \tag{5.5b}$$

where

$$\delta = \frac{\varepsilon_e \lambda_{Di}}{\varepsilon_i \lambda_{De}} \tag{5.6}$$

is the ratio of external to internal double-layer capacitance. The zeta potentials are defined as the potential drop from the interface to outside the double layer, and are

https://doi.org/10.1017/jfm.2011.288 Published online by Cambridge University Press

given by

$$\zeta_e(x) = \frac{E_0 x}{1+\delta}, \tag{5.7a}$$

$$\zeta_i(x) = -\frac{\delta E_0 x}{1+\delta}. \tag{5.7b}$$

The body forces exerted on the double layers are due to electrical force on the ions and the osmotic force established by the polarized double layer, which can be computed from (3.19). Thus, the body force on the external double layer is

$$\boldsymbol{f}_e = -\frac{\varepsilon_e}{\lambda_{De}^2}\zeta_e(x) E_0 \mathrm{e}^{-(y-d)/\lambda_{De}}\hat{\boldsymbol{x}}. \tag{5.8}$$

Since the liquid film is ideally polarizable and at steady state, the total potential inside the film is simply the internal double-layer potential, $\phi_{i,DL} = \phi_i$. Thus, the electric stress on the internal double layer is

$$\boldsymbol{f}_{i,ele} = -\rho_i \nabla \phi_i, \tag{5.9}$$

while the osmotic stress (from (3.15)) is

$$\boldsymbol{f}_{i,osm} = -k_B T \nabla (n_{i+} - n_{i-}) = \rho_i \nabla \phi_i. \tag{5.10}$$

Therefore, the electric stress and the osmotic pressure gradient are exactly equal and opposite, such that the total stress on the internal double layer is zero. This result is surprising, given that both free charge density and a non-zero tangential electric field are present within the internal double layer. Nonetheless, the two balance precisely.

The absence of internal electrokinetic stress means that the electrokinetic stress in the external double layer can only be balanced by the viscous stresses within the thin film. The $O(d/\lambda_D)$ velocity enhancement discussed in § 4 is therefore not limited to liquid metal interfaces, but occurs generally over ideally polarizable liquid interfaces. In particular, the effective electrokinetic slip velocity over a moderately conducting film with thin double layers is

$$u_s = -\frac{\varepsilon_e}{\eta_e}\frac{E_0^2 x}{1+\delta}\left(1 + \frac{1}{4}\frac{\eta_e}{\eta_i}\frac{d}{\lambda_D}\right), \tag{5.11}$$

which is completely analogous to (3.26)–(4.7), except with the induced $\zeta_e(x)$ reduced by a factor $(1+\delta)$ according to (5.7*a*).

Given that there is no electric field within the thin film, there can be no electro-osmotic flow over the film/solid interface. Therefore, the flow profile within the film is the same as that in the liquid metal film and is given by (4.5*b*).

We will now relax the assumption of a thin internal double layer and solve for the total electrostatic potential and body force with an equilibrium internal double layer of arbitrary thickness. Again, the total potential in each phase is given as a superposition of the external applied potential and the double layer potential (3.1). The double layer potentials obey the Poisson–Boltzmann equation (3.6), with dielectric boundary conditions at the interface (5.4). Far from the interface in the electrolyte, the total potential must decay to the applied potential (5.1). The wall boundary condition in the thin film requires that the potential at the metal surface be constant. Assuming the metal to be uncharged at equilibrium requires the wall potential to be set to zero:

$$\phi_i(x, 0) = 0. \tag{5.12}$$

https://doi.org/10.1017/jfm.2011.288 Published online by Cambridge University Press

The general solution for the applied potential in the electrolyte is given by (5.2*a*), while in the thin film, a more convenient form that satisfies the equipotential solution at the wall is

$$\phi_i(x, y) = C \sinh\left(\frac{y}{\lambda_{Di}}\right). \tag{5.13}$$

The dielectric boundary conditions (5.4) lead to a total potential in each phase of

$$\phi_e(x, y) = \left(\frac{E_0 x}{1 + \delta \tanh(d/\lambda_{Di})}\right) \mathrm{e}^{-(y-d)/\lambda_{De}} - E_0 x, \tag{5.14a}$$

$$\phi_i(x, y) = -\frac{\delta E_0 x \sinh(y/\lambda_{Di})}{\cosh(d/\lambda_{Di}) + \delta \sinh(d/\lambda_{Di})}, \tag{5.14b}$$

where δ is the capacitance ratio between electrolyte and liquid film double layers given by (5.6). The total body force on the external double layer is then given by

$$\boldsymbol{f}_e = \rho E_0 \hat{\boldsymbol{x}} = -\frac{\varepsilon_e}{\lambda_{De}^2}\left(\frac{E_0^2 x}{1 + \delta \tanh(d/\lambda_{Di})}\right) \mathrm{e}^{-(y-d)/\lambda_{De}} \hat{\boldsymbol{x}}. \tag{5.15}$$

The body force on the internal double layer is the sum of the force due to the electric field on the free charge density and the osmotic pressure gradient from the polarization of the double layer. The electric field in the internal double layer,

$$-\frac{\partial \phi_i}{\partial x} = \frac{\delta \sinh(y/\lambda_{Di})}{\cosh(d/\lambda_{Di}) + \delta \sinh(d/\lambda_{Di})} E_0, \tag{5.16}$$

drives the free charge density,

$$\rho = -\varepsilon_i \nabla^2 \phi_i = \frac{\varepsilon_i E_0 x}{\lambda_{Di}^2} \frac{\delta \sinh(y/\lambda_{Di})}{\cosh(d/\lambda_{Di}) + \delta \sinh(d/\lambda_{Di})}, \tag{5.17}$$

to exert an electrical body force of

$$\boldsymbol{f}_{ele} = \frac{\delta^2 \varepsilon_i E_0^2 x}{\lambda_{Di}^2} \frac{\sinh^2(y/\lambda_{Di})}{[\cosh(d/\lambda_{Di}) + \delta \sinh(d/\lambda_{Di})]^2} \hat{\boldsymbol{x}}. \tag{5.18}$$

The concentration of ions in the internal double layer follows from (3.16), which leads to an osmotic body force of

$$\boldsymbol{f}_{osm} = -k_B T \frac{\partial}{\partial x}(n_+ + n_-)\hat{\boldsymbol{x}} = -\frac{\delta^2 \varepsilon_i E_0^2 x}{\lambda_{Di}^2} \frac{\sinh^2(y/\lambda_{Di})}{[\cosh(d/\lambda_{Di}) + \delta \sinh(d/\lambda_{Di})]^2} \hat{\boldsymbol{x}}, \tag{5.19}$$

which is precisely equal and opposite to the electrical body force. The total body force, $\boldsymbol{f}_{ele} + \boldsymbol{f}_{osm}$, on the internal double layer is therefore identically zero, in general (figure 3*d*). Once again, the lack of an equal and opposite electrokinetic stress on the internal double layer implies a net electrokinetic stress on the interface that can only be balanced by viscous stresses within the flowing film. Therefore, the electrokinetic slip velocity over any ideally polarizable liquid interface is expected to follow Levich–Frumkin scaling.

The flow in the electrolyte and the thin film is completely analogous to that found for a thin liquid metal film in § 4, with the only difference being that applied potential drop from the bulk electrolyte to the metal surface is split across two double layers:

https://doi.org/10.1017/jfm.2011.288 Published online by Cambridge University Press

the zeta potential in the electrolyte,

$$\zeta_e(x) = \frac{E_0 x}{1 + \delta \tanh(d/\lambda_{Di})}, \tag{5.20}$$

where δ is given by (5.6), is the source of the electro-osmotic stress and drives the electrokinetic flow, while the remainder, as measured from the interface to the internal bulk,

$$\zeta_i(x) = -\frac{\delta \tanh(d/\lambda_{Di}) E_0 x}{1 + \delta \tanh(d/\lambda_{Di})}, \tag{5.21}$$

is dropped across the internal double layer, and does not generate a stress or drive an electrokinetic flow. This leads to a slip velocity in the bulk electrolyte far from the liquid/liquid interface of

$$u_s = -\frac{\varepsilon_e \zeta_e(x) E_0}{\eta_e} \left(1 + \frac{1}{4}\frac{\eta_e}{\eta_i}\frac{d}{\lambda_{De}}\right). \tag{5.22}$$

It is instructive to consider the limits of (5.22) for both thin ($\lambda_{Di} \ll d$) and thick ($\lambda_{Di} \gg d$) internal double layers. An infinitely thin internal double layer corresponds to the thin film behaving like a liquid metal. As $d/\lambda_{Di} \to \infty$, $\delta \tanh(d/\lambda_{Di}) \to \delta$, and (5.22) becomes

$$u_s(\lambda_{Di} \ll d) \to -\frac{\varepsilon_e E_0^2 x}{\eta_e \left[1 + \dfrac{\varepsilon_e}{\varepsilon_i}\dfrac{\lambda_{Di}}{\lambda_{De}}\right]} \left(1 + \frac{1}{4}\frac{\eta_e}{\eta_i}\frac{d}{\lambda_{De}}\right). \tag{5.23}$$

Furthermore, in the limit where the liquid film is significantly more conductive than the electrolyte ($\lambda_{Di} \ll \lambda_{De}$), (5.23) approaches the slip velocity over a liquid metal (4.6), as expected. Thus, the electrokinetic behaviour in the limit as $\lambda_{Di}/\lambda_{De}$ approaches zero is identical to the behaviour derived in the limit of a perfect liquid metal (where $\lambda_{Di} = 0$), revealing nothing singular about the liquid metal limit.

The opposite limit ($d/\lambda_{Di} \to 0$, with a finite d) corresponds to a non-conductive, purely dielectric thin film. In this case, $\delta \tanh(d/\lambda_{Di}) \to (\varepsilon_e d)/(\varepsilon_i \lambda_{De})$, to give a zeta potential in the electrolyte,

$$\zeta_e(x) \to \frac{E_0^2 x}{1 + \dfrac{\varepsilon_e d}{\varepsilon_i \lambda_{De}}}, \tag{5.24}$$

which is identical to the zeta potential over a solid dielectric found by Squires & Bazant (2004) and Pascall & Squires (2010*a*,*b*). Since the dielectric is liquid, however, the non-zero net stress exerted upon the interface is balanced by the viscous stress of the flowing film, whose moving interface enhances the total electro-osmotic slip (5.22) to give

$$u_s(\lambda_{Di} \gg d) \to -\frac{\varepsilon_e E_0^2 x}{\eta_e \left[1 + \dfrac{\varepsilon_e d}{\varepsilon_i \lambda_{De}}\right]} \left(1 + \frac{1}{4}\frac{\eta_e}{\eta_i}\frac{d}{\lambda_{De}}\right). \tag{5.25}$$

In the frequent limit where the permittivity and viscosity of electrolyte and film are comparable and the film is much thicker than the screening length in the electrolyte ($d \gg \lambda_{De}$), the zeta-potential suppression due to the dielectric capacitance (5.24) is

https://doi.org/10.1017/jfm.2011.288 Published online by Cambridge University Press

nearly compensated by the Frumkin–Levich enhancement so that (5.25) becomes

$$u_s(\lambda_{De} \ll d \ll \lambda_{Di}) \to -\frac{\varepsilon_e E_0^2 x}{4\eta_e}\left(\frac{\varepsilon_i \eta_e}{\varepsilon_e \eta_i}\right). \tag{5.26}$$

Thus, by suitably choosing the permittivity and viscosity of the liquid thin film, the induced charge electro-osmotic flow over a dielectric liquid thin film can be engineered to match that over a solid metal surface. Note, however, that (5.26) would be largely insensitive to dielectric contaminants of the electrode itself, unlike standard induced-charge electrokinetic (ICEK) flows over otherwise clean metal/electrolyte interfaces (Pascall & Squires 2010*a*,*b*).

While only the induced charge electro-osmotic flows have been explicitly computed in this section, an equilibrium zeta potential may be present across the external and internal double layers due to various mechanisms such as charge present at the liquid/liquid interface, specific adsorption of ions to the metal strip's surface, or by actively applying a potential to the metal strip. The net effect of any native equilibrium zeta potential can be considered by redefining the external zeta potential (5.7*a*) and (5.20) to be the sum of an external equilibrium zeta potential and the induced zeta potential. The body force in the external double layer and the slip velocity are still given by (5.8) and (5.22), respectively. Thus, the only difference between the flow over an ideally polarizable thin film of a general liquid and a thin film of liquid metal (given equivalent physical properties) is that the induced zeta potential (and thus the induced charge electro-osmotic component of the flow) over a general liquid is reduced by a factor $[1 + \delta \tanh(d/\lambda_{Di})]^{-1}$ due to the potential dropped across the thin film.

The velocity enhancement arises here for precisely the same reason that it did in the liquid metal thin film: the lack of an equal and opposite electrokinetic stress in the internal double layer yields a non-zero total stress on the interface that can only be balanced by viscous stresses in the (flowing) thin film. The lack of an electro-osmotic stress in the internal double layer is surprising given that a tangential electric field exists in the double layer. However, the electric stress that this field generates is exactly balanced by an osmotic pressure gradient established by the polarized double layer. This is a direct result of the double layer being equilibrated with the adjacent bulk electrolyte, as will be shown in the next section.

6. Relating the body force on the double layer to the electrochemical potential

In the previous section, we have shown in a variety of systems that the electro-osmotic body force in external double layers is simply the product of the free charge density and the applied field, $\rho E_\parallel$. However, for the internal double layer, the electric stress exactly cancels the osmotic pressure gradient giving a net stress-free double layer. This remarkable result is not obvious *a priori*. In this section, we use the electrochemical potential to show that this cancellation is a direct consequence of the quasi-equilibrium structure of the double layer.

We begin by defining the electrochemical potential of an ion species, i, in the dilute limit as

$$\mu_i \equiv k_B T \log n_i + z_i e\phi + \mu_i^o, \tag{6.1}$$

where z_i is the signed valence of the ith ion and μ_i^o is a reference chemical potential. The gradient of the electrochemical potential represents the total force exerted on the ion. The first term of (6.1) gives rise to an entropic force, $\boldsymbol{f} = -k_B T \nabla \log n_i$, that tends

https://doi.org/10.1017/jfm.2011.288 Published online by Cambridge University Press

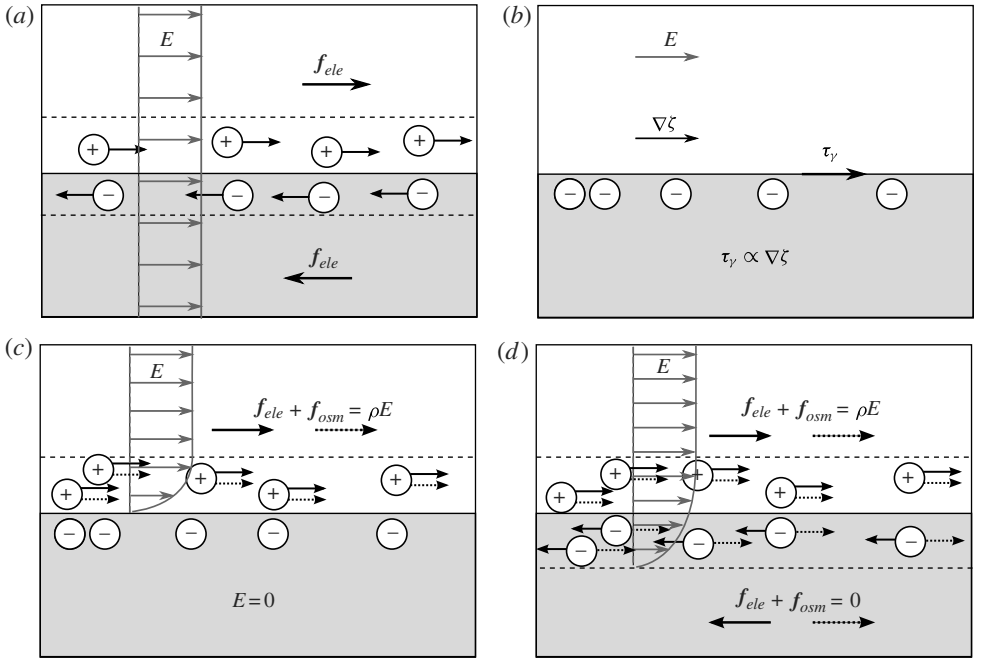


FIGURE 3. The forces exerted on the double layers for the scenarios presented in this article. (*a*) Booth's neglect of double-layer polarization leads an approximately constant electric field across the double layer. Thus, for thin double layers, the electrical force applied to the external double layer is exactly counterbalanced by the electrical force on the internal double layer, leading to zero net stress on the interface. (*b*) Frumkin and Levich did not explicitly compute the forces on the double layer but rather posited that the gradient in zeta potential around a conductive drop leads to a Marangoni stress, $\boldsymbol{\tau}_\gamma$, at the interface given by the Lippmann–Helmholtz equation (4.8). (*c*) Explicitly computing the forces on the ions in the double layer near a conductive surface reveals that the total force arises from both the force exerted by the electric field on the ions, $\boldsymbol{f}_{ele}$, and that from the osmotic pressure gradient, $\boldsymbol{f}_{osm}$. Furthermore, the total force is given by the product of the free charge density and the external tangential electric field. (*d*) Extending the computation of forces to ions in an internal double layer reveals that the electrical force and osmotic force are exactly equal and opposite. Thus, there is no net force applied on internal double layers (6.2).

to force the ion down concentration gradients, while the second term is the source of the electrostatic force on the ions, $\boldsymbol{f} = -z_i e \boldsymbol{\nabla}\phi$.

Chu & Bazant (2007) and the references therein showed that the thin-double-layer approximation implies that the double layer is in quasi-equilibrium with the adjacent bulk. As such, the chemical potentials $\mu_i(x, y)$ are constant across the double layer, $\mu_i(x, y) = \mu_i(x)$, so that equilibrated ions move freely back and forth across the double layer. Since $\mu(x)$ is constant across the double layer, the only gradients (forces) that arise are directed along the double layer. In particular, the tangential gradient, $-\boldsymbol{\nabla}_x \mu_i$, which gives the force on each ion at any point in the double layer, is identical to the tangential gradient at any other location across the double layer. Thus, one can evaluate this tangential force on an ion in the bulk ($y \to \infty$), beyond the double layer, where its form is particularly simple (here $\boldsymbol{\nabla}_x \mu_i^\infty \to z_i e E_\parallel$), and know that ions of the same charge within the double layer experience the same force. The total body force, then, is given by the force per ion ($-\boldsymbol{\nabla}_x \mu_i$) times the excess local concentration of

https://doi.org/10.1017/jfm.2011.288 Published online by Cambridge University Press

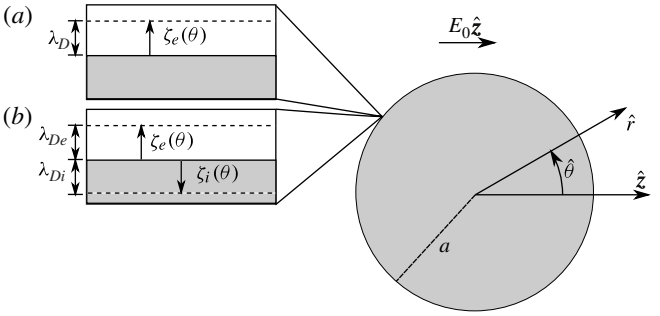


FIGURE 4. A liquid drop suspended in an electrolyte. An electric field, $\boldsymbol{E} = E_0\hat{\boldsymbol{z}}$, is applied far from the drop. Due to the fact that $\lambda_D \ll a$, the double layer around the drop appears locally planar with an angle dependent zeta potential, $\zeta_e(\theta)$. (*a*) In the case of a liquid metal drop, the applied potential is dropped entirely across an external double layer. (*b*) For a drop of moderate conductivity, the applied potential drop is split between the external and internal double layers. Regardless of the drop's conductivity, an ideally polarizable drop translates with a velocity $\boldsymbol{U} = [\varepsilon_e\zeta_0\boldsymbol{E}/(3\eta_i + 2\eta_e)][(a/\lambda_D) + (3\eta_i/\eta_e) + 1]$, where ζ_0 is the native equilibrium zeta potential of the external double layer.

ions $[n_i(x, y) - n_0]$:

$$\begin{aligned} \boldsymbol{f}_{tot}(x, y) &= -\sum_i \nabla_x \mu_i(x)[n_i(x, y) - n_0] \\ &= E_\parallel(x) \sum_i z_i e[n_i(x, y) - n_0] \\ &\equiv \rho(x, y)E_\parallel(x), \end{aligned} \tag{6.2}$$

where $E_\parallel$ is the component of the applied electric field tangent to the surface.

Thus, the body force on a fluid element in an equilibrated double layer, whose electrochemical potential is constant across the double layer, is always the product of the local free charge density and the applied electric field present in the bulk. The fact that the electrochemical potential is constant across the double layer thus reveals the reason for what had seemed to be a fortuitous cancellation of electrical and osmotic forces: polarizing a near-equilibrium double layer gives rise to gradients in electrical potential energy that are compensated by equal and opposite gradients in entropy. Only when a tangential gradient of the electrochemical potential outside a double layer exists – which drives, for example, a steady non-equilibrium ion flux – will there be a non-zero electrokinetic stress on the double layer. A simple consequence of the near-equilibrium nature of polarized double layers is that internal double layers, beyond which $\boldsymbol{E} = \boldsymbol{0}$ due to the closed and steady-state nature of the drop or film, experience identically zero tangential stress.

The next section revisits the classical problem studied by Frumkin (1946): the electrophoresis of a liquid metal drop. The framework presented in this section will be used to calculate the body force on the double layer and the corresponding flow in the electrolyte and drop. We will show that that the velocity enhancement predicted by Frumkin (1946) arises from the stresses present in a relaxed, polarized double layer and the lack of corresponding stresses in the metal drop.

https://doi.org/10.1017/jfm.2011.288 Published online by Cambridge University Press

7. Revisiting the electrophoresis of a liquid metal drop

In this section, we reconsider the electrophoretic mobility of a liquid drop (Henry 1931; Frumkin 1946; Levich 1962; Levine & O'Brien 1973). Here, a liquid metal drop of radius, a, and viscosity, η_i, is freely suspended in an electrolyte with permittivity, ε_e, and viscosity, η_e. We adopt a spherical coordinate system whose origin is fixed to the centre of the drop such that the interface is located at $r = a$ (figure 4). We work in the thin-double-layer limit where $\lambda_D \ll a$ with the assumption that the interface is ideally polarizable. An electric field, $E_0\hat{\boldsymbol{z}}$, is applied in the bulk of the electrolyte, causing the drop to translate with a velocity, $\boldsymbol{U}$. The native zeta potential of the drop, ζ_0, is such that the total zeta potential is low ($\zeta_0 + E_0 a \ll k_B T/ez$). We further assume that the drop does not deform while translating. In order to determine the translational velocity of the drop, we follow the now familiar procedure of computing the electrostatic potential in the electrolyte from which the body force on the double layer is calculated, followed by the electro-osmotic flow in both the electrolyte and drop.

The total potential in the electrolyte is the superposition of the applied potential from the external electric field and the double layer potential near the interface (3.1). The applied potential obeys Laplace's equation (3.3) in the electrolyte. At steady state, the far-field boundary condition requires that the applied potential gives the applied field far from the drop,

$$\phi_{app}(r \to \infty, \theta) \to -E_0 r \cos\theta. \tag{7.1}$$

The boundary condition at the drop's surface requires that there is no current normal to the interface:

$$\left.\frac{\partial \phi_{app}}{\partial r}\right|_{r=a} = 0. \tag{7.2}$$

This results in an applied potential of

$$\phi_{app}(r, \theta) = -E_0 r \cos\theta \left(1 + \frac{a^3}{2r^3}\right). \tag{7.3}$$

The double layer potential obeys the Poisson–Boltzmann equation (3.6) with the boundary conditions

$$\phi_{DL}(r \to \infty, \theta) \to 0, \tag{7.4a}$$

$$\phi_{DL}(a, \theta) = \zeta_0 + \tfrac{3}{2} E_0 a \cos\theta. \tag{7.4b}$$

Due to the assumption of a thin double layer with respect to the radius of the drop, gradients of the double layer potential in the θ-direction are $O(\lambda_D^2)$ smaller than gradients in the radial direction, and are therefore neglected. However, as will be shown below, the $O(\lambda_D)$ radial term that accounts for the curvature of the interface must be retained as it leads to a term that produces a velocity that is of the same order as the electro-osmotic flow in the double layer. Therefore, the double-layer potential is

$$\phi_{DL}(r, \theta) = \zeta_e(\theta) \left(\frac{a}{r}\right) \mathrm{e}^{-(r-a)/\lambda_D}, \tag{7.5}$$

such that the total potential is

$$\phi(r, \theta) = \zeta_e(\theta) \left(\frac{a}{r}\right) \mathrm{e}^{-(r-a)/\lambda_D} - E_0 r \cos\theta \left(1 + \frac{a^3}{2r^3}\right), \tag{7.6}$$

https://doi.org/10.1017/jfm.2011.288 Published online by Cambridge University Press

where

$$\zeta_e(\theta) \equiv \zeta_0 + \tfrac{3}{2} E_0 a \cos\theta. \tag{7.7}$$

The body force on the double layer can be found directly from (6.2). The free charge density is

$$\rho = -\frac{\varepsilon_e}{\lambda_D^2} \zeta_e(\theta) \left(\frac{a}{r}\right) \mathrm{e}^{-(r-a)/\lambda_D}, \tag{7.8}$$

while the tangential applied field at the surface is

$$E_t = -\hat{\boldsymbol{\theta}} \cdot \nabla \phi_{app}(a, \theta) = -\tfrac{3}{2} E_0 \sin\theta, \tag{7.9}$$

which gives a body force in the double layer of

$$\boldsymbol{f} = \frac{3\varepsilon_e \zeta_e(\theta) E_0}{2\lambda_D^2} \left(\frac{a}{r}\right) \mathrm{e}^{-(r-a)/\lambda_D} \sin\theta \hat{\boldsymbol{\theta}}. \tag{7.10}$$

Since the metal cannot support any electric field, there is no body force inside the drop.

The flow both in the drop and in the electrolyte is governed by the incompressible Stokes equations (3.20). Due to the large scale difference between the drop radius and the double-layer thickness, the electro-osmotic flow in the double layer will be solved separately from the flow in the bulk electrolyte and drop. The electro-osmotic flow will manifest itself as jumps in velocity and shear stress across the interface in the bulk flow problem.

The flow in the double layer is computed by integrating the Stokes equations from the interface to the bulk with the body force term given by (7.10). This yields a velocity difference

$$\Delta \boldsymbol{U}(\theta) = \frac{3\varepsilon_e}{2\eta_e} \zeta_e(\theta) E_0 \sin\theta \tag{7.11}$$

across the double layer due to electro-osmosis. The body force on the double layer is accounted for in the bulk problem by an additional shear stress at the interface. This stress is the integrated body force across the double layer:

$$\tau(\theta) = \frac{1}{a^2} \int_a^\infty \hat{\boldsymbol{\theta}} \cdot \boldsymbol{f} r^2 \, \mathrm{d}r = \frac{3\varepsilon_e}{2\lambda_D} \left(1 + \frac{\lambda_D}{a}\right) \zeta_e(\theta) E_0 \sin\theta. \tag{7.12}$$

The $O(\lambda_D/a)$ term that results from the curvature of the interface must be retained even in the thin-double-layer limit as it leads to a contribution to the translational velocity that is of the same order as the electro-osmotic flow present in the double layer.

The bulk electrolyte and drop obey the unforced Stokes equations, and the flow in each is coupled at the interface:

$$u_{\theta,e}(a, \theta) - u_{\theta,i}(a, \theta) = \Delta \boldsymbol{U}(\theta), \tag{7.13a}$$

$$u_{r,e}(a, \theta) = u_{r,i}(a, \theta) = 0, \tag{7.13b}$$

$$\tau_{r\theta,e}|_{r=a} - \tau_{r\theta,i}|_{r=a} = \tau(\theta). \tag{7.13c}$$

The boundary conditions far from the interface require that the flow in the electrolyte approaches a constant,

$$u_e(r \to \infty, \theta) = -U\hat{\boldsymbol{z}} \tag{7.14}$$

https://doi.org/10.1017/jfm.2011.288 Published online by Cambridge University Press

and that the velocities in the drop remain bounded. The constant velocity, $\boldsymbol{U}$, is the object of the calculation. Additionally, the motion of the drop is force-free. These boundary conditions lead to a stream function solution

$$\psi_e(r,\theta) = \frac{1}{2}\frac{\varepsilon_e E_0 \zeta_0 a^2}{3\eta_i + 2\eta_e}\left(\frac{a}{\lambda_D} + \frac{3\eta_i}{\eta_e} + 1\right)\left(\frac{r^2}{a^2} - \frac{a}{r}\right)\sin^2\theta + \frac{9}{40}\frac{\varepsilon_e E_0^2 a^3}{\eta_i + \eta_e}\left(\frac{a}{\lambda_D} + \frac{5\eta_i}{\eta_e} + 1\right)\left(1 - \frac{a^2}{r^2}\right)\sin^2\theta\cos\theta, \tag{7.15}$$

for the electrolyte, and

$$\psi_d(r,\theta) = \frac{3}{4}\frac{\varepsilon_e E_0 \zeta_0 a^2}{3\eta_i + 2\eta_e}\left(\frac{a}{\lambda_D} - 1\right)\left(\frac{r^4}{a^4} - \frac{r^2}{a^2}\right)\sin^2\theta + \frac{9}{40}\frac{\varepsilon_e E_0^2 a^3}{\eta_i + \eta_e}\left(\frac{a}{\lambda_D} - 4\right)\left(\frac{r^5}{a^5} - \frac{r^3}{a^3}\right)\sin^2\theta\cos\theta, \tag{7.16}$$

for the drop, where the velocity is related to the stream function by

$$u_r = \frac{1}{r^2\sin\theta}\frac{\partial\psi}{\partial\theta}, \quad u_\theta = -\frac{1}{r\sin\theta}\frac{\partial\psi}{\partial r}. \tag{7.17}$$

Thus, the drop translates with an electrophoretic velocity,

$$\boldsymbol{U} = \frac{\varepsilon_e \zeta_0 \boldsymbol{E}}{3\eta_i + 2\eta_e}\left(\frac{a}{\lambda_D} + \frac{3\eta_i}{\eta_e} + 1\right), \tag{7.18}$$

which is identical to that reported by Ohshima *et al.* (1984) and Ohshima (1997) in the thin-double-layer, low-zeta-potential limit.

In this expression, the second term represents standard electrophoresis (as if the drop were insulating), as computed by Booth (1951), whereas the first $[O(a/\lambda_D)]$ and third $[O(1)]$ terms arise from the polarization of the double layer. The dominant $[O(a/\lambda_D)]$ term is identical to that calculated by Levich (1962), whose electrocapillary approach relies on thermodynamic properties of the interface, and thus neglects any subdominant $[O(1)]$ term due to the electro-osmotic velocity jump entirely. Additionally, any finite double-layer thickness modifies the double-layer capacitance by $O(\lambda_D/a)$, which thus changes the electrocapillary stress (7.12) by $O(\lambda_D/a)$, to give an $O(1)$ contribution to the translational velocity (7.18) that cannot be safely neglected as it is of the same order as the electro-osmotic velocity. In our analysis, contributions from both polarization and standard electrophoresis arise naturally and intuitively by correctly accounting for the gradients in chemical potential along the interface.

The analysis presented in § 5 for conductive dielectric thin films can be adapted to find the translational velocity of a dielectric drop. Suppose that the drop is composed of a conductive dielectric liquid with permittivity, ε_i, and is charged such that the potential in the bulk of the drop is ϕ_d relative to the bulk electrolyte. We will again assume that the double layers are thin, the zeta potentials are low, and the interface is ideally polarizable. At steady state, there cannot be an electric field within the drop. Thus the total potentials both outside and inside the drop are

$$\phi_e(r,\theta) = \left(\zeta_0 + \frac{3}{2(1+\delta)}E_0 a\cos\theta\right)\left(\frac{a}{r}\right)\mathrm{e}^{-(r-a)/\lambda_{De}} - \frac{3}{2}E_0 a\cos\theta, \tag{7.19a}$$

$$\phi_i(r,\theta) = -\left(\delta\zeta_0 + \frac{3\delta}{2(1+\delta)}E_0 a\cos\theta\right)\mathrm{e}^{(r-a)/\lambda_{Di}} + \phi_d, \tag{7.19b}$$

https://doi.org/10.1017/jfm.2011.288 Published online by Cambridge University Press

where δ is given by (5.6), and the native zeta potential is related to the drop's potential by

$$\zeta_0 = \frac{\phi_d}{1+\delta}. \tag{7.20}$$

While the effects of curvature must be retained for the external potential in the thin-double-layer limit for the reasons mentioned above, there is no such requirement for the internal potential, as the internal double layer is force-free (6.2):

$$\boldsymbol{f} = -\rho_i \nabla \phi_d = 0. \tag{7.21}$$

Solving for the flow in the electrolyte and drop in an analogous manner to the liquid metal drop gives

$$\begin{aligned}\psi_e(r,\theta) = {} & \frac{1}{2}\frac{\varepsilon_e E_0 \zeta_0 a^2}{3\eta_i + 2\eta_e}\left(\frac{a}{\lambda_D} + \frac{3\eta_i}{\eta_e} + 1\right)\left(\frac{r^2}{a^2} - \frac{a}{r}\right)\sin^2\theta \\ & + \frac{9}{40}\frac{\varepsilon_e E_0^2 a^3}{(1+\delta)(\eta_i+\eta_e)}\left(\frac{a}{\lambda_D} + \frac{5\eta_i}{\eta_e} + 1\right)\left(1 - \frac{a^2}{r^2}\right)\sin^2\theta\cos\theta, \end{aligned} \tag{7.22}$$

for the electrolyte, and

$$\begin{aligned}\psi_d(r,\theta) = {} & \frac{3}{4}\frac{\varepsilon_e E_0 \zeta_0 a^2}{3\eta_i + 2\eta_e}\left(\frac{a}{\lambda_D} - 1\right)\left(\frac{r^4}{a^4} - \frac{r^2}{a^2}\right)\sin^2\theta \\ & + \frac{9}{40}\frac{\varepsilon_e E_0^2 a^3}{(1+\delta)(\eta_i+\eta_e)}\left(\frac{a}{\lambda_D} - 4\right)\left(\frac{r^5}{a^5} - \frac{r^3}{a^3}\right)\sin^2\theta\cos\theta\,, \end{aligned} \tag{7.23}$$

for the drop. Thus, the only difference between a liquid metal drop and a liquid conductive dielectric drop is that the induced charge electro-osmotic flow around the dielectric drop is suppressed by a factor $(1+\delta)^{-1}$. Both drops translate with the velocity given by (7.18).

Levine & O'Brien (1973) correctly noted that polarization of the double layer is a key requirement for the enhanced electrokinetic mobility of liquid metal drops, but the mechanism by which this occurs is not clear from their analysis. Furthermore, the generalization of their argument to non-infinitely conducting drops is not straightforward. In particular, Levine & O'Brien (1973) explicitly (and correctly) impose a zero electrical stress inside the liquid metal drop, such that electrokinetic stresses external to the drop can only be balanced by viscous stresses due to internal circulation. Levine & O'Brien (1973) effectively reproduced the work of Booth (1951) by neglecting polarization, which leads to a tangential electric field that is continuous across the interface, such that the net stress $-\sigma_0 E_\parallel$ on the external double layer (with charge density σ_0) is balanced to leading order in a/λ_D by an equal and opposite stress $\sigma_0 E_\parallel$ on the surface charge at the interface. The Levich–Frumkin scaling, which arises when net $O(\sigma_0 E)$ electrokinetic stresses on the interface are balanced by $O(\eta U/a)$ viscous stresses, thus does not occur. Corrections due to finite double-layer thickness are smaller by $O(\lambda_D/a)$; therefore, internal circulation (and thus the electrophoretic mobility) is smaller than Levich–Frumkin's by $O(\lambda_D/a)$, consistent with Booth (1951).

Here, by contrast, we have shown much more generally that the central physical mechanism behind the Levich–Frumkin scaling is the existence of a net electrokinetic stress on the liquid/liquid/double-layer(s) interface. Furthermore, we have shown that non-zero electrokinetic interfacial stresses arise quite generally around ideally polarizable interfaces regardless of the conductivity of the abutting liquid phases.

https://doi.org/10.1017/jfm.2011.288 Published online by Cambridge University Press

In steady state, the double layer internal to a closed, ideally polarizable volume of fluid experiences identically zero electrokinetic stress, as electrical and osmotic stresses precisely cancel. This result follows from the quasi-equilibrium structure of the internal double layer, wherein the chemical potential gradient in the bulk (which is zero in the internal double layer) is identical to the chemical potential gradient at the interface (§ 6).

8. The effects of surface conduction

Our analysis to this point has neglected the influence of electrical currents within the double layers. Ohshima *et al.* (1984), however, showed that the velocity enhancement predicted by Frumkin (1946) occurs only at low zeta potentials. At higher zeta potentials, the mobility of the liquid metal drop approaches that of rigid particles, an effect Ohshima *et al.* (1984) termed 'solidification'. Both Ohshima *et al.* (1984) and Baygents & Saville (1991) recognize that this need not be due to a solid film at the interface, but rather to the increasing importance of inhomogeneous surface transport around the curved particle surface (O'Brien & White 1978; Dukhin 1993; Khair & Squires 2009*a*).

More generally, charge and shape inhomogeneities drive inhomogeneous surface transport, which can cause qualitative changes in electrokinetic behaviour. The relative importance of surface conduction is parametrized by the Dukhin number,

$$Du = \frac{\sigma_s}{\sigma_b l}, \tag{8.1}$$

which represents the relative importance of the surface current, $\boldsymbol{j_s} = \sigma_s \boldsymbol{E}$, to the bulk current, $\boldsymbol{j_b} = \sigma_b \boldsymbol{E}$, with a geometric length scale l (Lyklema 1995). In the planar electrode geometries studied here, electro-osmotic flow gradients occur over a length scale given by the electrode half-width $l = L/2$.

The surface current is defined in terms of the excess current in the electrolyte due to the double layer (Lyklema 1995):

$$\boldsymbol{j}_s \equiv \int_0^\infty \boldsymbol{j}(y) - \boldsymbol{j}(\infty)\,\mathrm{d}y, \tag{8.2}$$

where the bulk current is

$$\boldsymbol{j}(\infty) = \sigma_b \boldsymbol{E}. \tag{8.3}$$

For a symmetric $z:z$ electrolyte, the current density is given by

$$\boldsymbol{j}(y) = ez(n_+ \boldsymbol{v}_+ - n_- \boldsymbol{v}_-), \tag{8.4}$$

where

$$\boldsymbol{v}_\pm = \pm \frac{De\,z}{k_B T} \boldsymbol{E} - u_x(x, y) \tag{8.5}$$

is the velocity at which an ion moves through the fluid and D is the ion's diffusivity. The first term in (8.5) represents the electromigrative velocity of the ion being forced through the fluid, while the second term represents the convection of the ion along with the electro-osmotic flow. In the case of the solid metal strip, $u_x(x, y)$ is given by (3.21), which leads to a surface current of

$$\boldsymbol{j}_s = 8\lambda_D (1 + m) \sinh^2\left(\frac{ez\zeta(x)}{4k_B T}\right) \sigma_B \boldsymbol{E}, \tag{8.6}$$

https://doi.org/10.1017/jfm.2011.288 Published online by Cambridge University Press

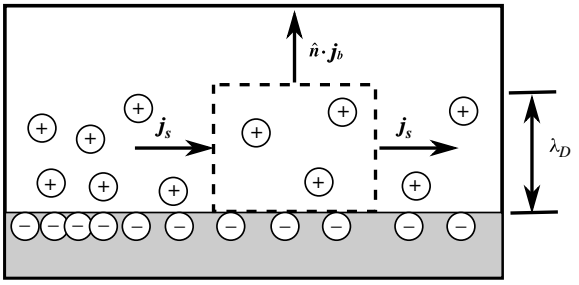


FIGURE 5. Changes in the current along the surface of the interface, $\boldsymbol{j_s} = \sigma_s \boldsymbol{E}_{\parallel}$, are balanced by the current supplied from the bulk, $\hat{\boldsymbol{n}} \cdot \boldsymbol{j_b} = \sigma_b E_{\perp}$. The relative importance of surface current to bulk current is characterized by the Dukhin number, $Du = \sigma_s/\sigma_b l$, where l is the characteristic length scale over which gradients in surface current $\boldsymbol{j_s}$ occur.

where $m = 2\varepsilon_e (k_B T/ez)^2/\eta_e D$ reflects the relative importance of electroconvective to electromigrative ion transport. By (8.1), the Dukhin number for a solid, metallic strip is thus given by

$$Du_{no\text{-}slip} = \frac{4\lambda_D}{l}(1+m)\sinh^2\left(\frac{ez\zeta(x)}{4k_B T}\right). \tag{8.7}$$

Since ions are conserved, a current balance on an element containing the double layer (figure 5) requires surface current variations to be balanced by flux to and from the bulk:

$$\hat{\boldsymbol{n}} \cdot \boldsymbol{j_b} = -\nabla_s \cdot \boldsymbol{j_s}, \tag{8.8}$$

where $\nabla_s = (\boldsymbol{I} - \hat{\boldsymbol{n}}\hat{\boldsymbol{n}}) \cdot \nabla$ is the surface divergence operator. As can be seen in figure 5, gradients in surface current require ions be supplied to, or removed from, the double layer. This requires non-zero electric fields normal to the double layer, which reduce the magnitude of the tangential component, and thus the electro-osmotic flow itself.

In the planar geometries here, surface current variations occur due to both the variations in ζ along the film, as well as the abrupt ζ discontinuity at the edge of the film. Khair & Squires (2008*b*) extended Yariv's (2004) work on step discontinuities to higher surface charge by considering the effects of ion conservation at the charge discontinuity, and found that the electrokinetic flow is suppressed over a 'healing length' of order lDu, or σ_s/σ_B, from the discontinuity. Analogous discontinuities are found in patchy, superhydrophobic surfaces, for which Zhao (2010) showed that finite-Du effects reduce the slip-enhanced velocities predicted by Squires (2008) and Bahga *et al.* (2010).

Additionally, surface conduction can lead to bulk concentration polarization over inhomogeneous charged surfaces (Dukhin 1993; Khair & Squires 2008*a*). Such effects are particularly strong in systems with relatively high surface area, for example at junctions between micro- and nanochannels (Bocquet & Charlaix 2010), due to the exclusion of coions within the nanochannel. This has been exploited by Wang, Stevens & Han (2005) to produce a filter that concentrates peptides, and by Kim *et al.* (2010) as the basis of a continuous desalinator, while Mani, Zangle & Santiago (2009) and Zangle, Mani & Santiago (2009) showed that concentration polarization can propagate as shocks in the microchannel under certain conditions. Concentration polarization within a nanochannel can be further manipulated by patterning the surface charge on the wall (Daiguji, Oka & Shirono 2005), which allowed Karnik *et al.*

https://doi.org/10.1017/jfm.2011.288 Published online by Cambridge University Press

(2007) and Vlassiouk, Smirnov & Siwy (2008) to create nanofluidic diodes, and Leinweber & Tallarek (2005) and Leinweber *et al.* (2006) to effect plumes with strong concentrations of electrolyte.

In the present context, concentration polarization drives chemiosmotic flows that oppose the electro-osmotic flow, further reducing the flow over the surface (O'Brien 1983; Khair & Squires 2009*a*). Both the reduced tangential field and this back-chemiosmotic component cause the non-monotonic mobility with respect to zeta potential that was found by O'Brien & White (1978), O'Brien (1983) and Dukhin (1993) for the electrophoresis of spherical colloids, by Messinger & Squires (2010) for electro-osmosis over rough solid surfaces, by López-García, Aranda-Rascón & Horno (2008) and Khair & Squires (2009*b*) when ion steric effects are incorporated, and by Baygents & Saville (1991), Ohshima *et al.* (1984) and Ohshima (1997) for the 'solidification' of liquid drops.

Khair & Squires (2009*a*) examined the electrophoresis of charged spheres with finite solid/liquid slip, which specifically isolates the influence of an enhanced convective velocity of the double layer. They found that solid–liquid slip enhances the electro-osmotic slip velocity, but also the surface conductivity compared to a no-slip sphere under the same conditions. They showed all thin-double-layer results to collapse onto a single, master curve when the electrophoretic mobility (scaled by its low-*Du* limit) was plotted against a suitably modified Dukhin number that included the electroconvective component. Khair & Squires (2009*b*) also demonstrated the same collapse for double layers with steric ions, again with an appropriately modified Dukhin number. These results reveal the central role played by the appropriate Dukhin number in determining electrokinetic velocities.

The electrokinetic velocity enhancements at liquid/liquid interfaces discussed above, then, require the appropriate Dukhin number to be small. For the liquid metal strip, $u_x(x, y)$ is given by (4.5*a*), which adds an additional electroconvective contribution,

$$Du_{liq\text{-}metal} = Du_{no\text{-}slip} + m\left(\frac{\eta_e d}{\eta_i l}\right)\sinh^2\left(\frac{ez\zeta(x)}{4k_BT}\right). \tag{8.9}$$

Notably, the moving liquid/liquid interface introduces a new contribution of order d/l to Du, which is thus $O(d/\lambda_{De})$ larger than $Du_{no\text{-}slip}$ (8.7). Although liquid metal surfaces can indeed enhance electrokinetic effects, the moving interface also enhances the electroconvective contribution to Du substantially relative to no-slip metal surfaces so that electro-osmotic flows are more readily suppressed, just as with partial-slip surfaces (Khair & Squires 2009*a*). This is consistent with the studies of Ohshima *et al.* (1984), who showed that 'solidification' sets in at relatively low ζ.

The surface conductivity over dielectric liquid films is enhanced in analogous fashion,

$$Du_{liq\text{-}diel} = Du_{no\text{-}slip} + m\left(\frac{\eta_e d}{\eta_i l}\right)\sinh^2\left(\frac{ezEx}{4k_BT[1+\delta\tanh(d/\lambda_{Di})]}\right), \tag{8.10}$$

although the argument of the sinh is now lower by an amount of order δ. Thus, although dielectric liquid films enhance ICEO flows less than liquid metal films do, the effective ICEO velocity (5.26) is driven by a rather low induced zeta potential (5.24), which therefore establishes a low Dukhin number. Thus, dielectric liquid coatings may provide a means of generating strong ICEK flows, while keeping Du low enough to avoid flow suppression due to surface conduction.

https://doi.org/10.1017/jfm.2011.288 Published online by Cambridge University Press

Finally, we now examine our earlier assertion that there can be no current or bulk field within closed, thin films whose surfaces are ideally polarizable. This is not strictly true: liquid/liquid interfaces, moving with velocity $U \sim \tau_e d/\eta_i$, convect any (internal) double layers, with surface charge density q_i, to drive a streaming current $I_i \sim q_i \tau_e d/\eta$. This internal streaming current must be balanced in steadystate by an equal and opposite current $I_{back} = -I_i$ within the film. A streaming potential, and thus back field $E_{back} = I_{back}/(\sigma_{B,i} d + \sigma_{s,i})$, must thus be established to drive this current. This back field, in turn, exerts an electrical stress $\tau_i = q_i E_{back}$ in a direction against the original electrokinetic stress on the external double layer. If this (opposing) internal stress were to have the same magnitude as the (external) driving stress, then any Levich–Frumkin enhancement would be lost. If, on the other hand, the internal stress were to be much weaker, then the Levich–Frumkin enhancement would hold, with only minor corrections.

The ratio of the 'streaming stress' to the driving stress is given by

$$\frac{\tau_i}{\tau_e} \sim \frac{q_i^2 d}{\eta(\sigma_i d + \sigma_{s,i})} = \frac{q_i^2}{\eta \sigma_i} \frac{1}{1 + Du_i}, \tag{8.11}$$

where $Du_i = \sigma_{s,i}/(\sigma_{B,i} d)$ is an internal Dukhin number. In the low-ζ_i (and $Du_i \ll 1$) limit, this stress ratio can be shown to be

$$\frac{\tau_i}{\tau_e}(Du_i \ll 1) \sim \frac{3}{2}\left(\frac{e\zeta_i}{k_B T}\right)^2 \frac{a_i}{\lambda_B}, \tag{8.12}$$

where a_i is the counter-ion radius and $\lambda_B = e^2/4\pi\varepsilon k_B T$ is the Bjerrum length in the film. Significantly, the internal stress is smaller than the driving stress by an amount of order ζ_i^2, where one power of ζ comes from the interfacial velocity, and the other from the charge density that is convected. In the low-ζ limit, then, the internal current can be safely neglected, as we have done throughout this work. In the high-ζ_i limit, (8.11) still holds; however, $q_i \sim \varepsilon/\lambda_{Di}(k_B T/e)^2 \sinh^2(e\zeta_i/2k_B T)$, and $Du_i \sim \sinh^2(e\zeta_i/2k_B T)$, giving

$$\frac{\tau_i}{\tau_e}(Du_i \gg 1) \sim \frac{a_i}{\lambda_B}, \tag{8.13}$$

which could either be small or $O(1)$, depending on the composition of the film. While these internal streaming currents, and associated back stress, are weak in the relatively low ζ_i limits considered in this manuscript, we defer a more detailed study of these internal currents and their implications for liquid-enhanced electrokinetics to future work.

9. Concluding remarks

We have revisited the problem of electrokinetics at liquid/liquid interfaces. By considering the electro-osmotic flow over a thin liquid metal film, we found that the key feature leading to Frumkin and Levich's prediction of a velocity enhancement was the presence of an unbalanced electro-osmotic stress at the interface. In the case of the liquid metal, it is unsurprising that such an unbalanced stress exists given that the metal can support no electric field. We showed, however, the unbalanced electric stress to be a general feature present even in liquids with vanishingly small conductivities. We explicitly showed the near-equilibrium nature of the internal double layer to result in identically zero internal electrokinetic stress. Since there is no steady state electric

https://doi.org/10.1017/jfm.2011.288 Published online by Cambridge University Press

field inside a closed, ideally polarizable drop or film, the net internal electrokinetic stress must vanish.

Despite the generality of these enhancements, there exist various mechanisms which lead to a balancing stress at the liquid/liquid interface, and thus the velocity enhancements predicted here may not be expected universally. As described in § 8, conduction of ions along the double layer is also enhanced in real systems with finite Debye lengths. Driving these surface currents necessitates supplying ions to the double layer from the bulk, which lowers the tangential field available to drive electro-osmotic flows. More generally, any mechanism that allows the interface itself to balance the electrical stress in the electrolyte, such as gradients in adsorbed surfactants or the formation of a solid film (e.g. the oxide layer formed by liquid gallium (Larsen *et al.* 2009; So & Dickey 2011)), will suppress the mobility enhancements discussed here. Indeed, even ions adsorbed to the interface from the electrolytes themselves may exert a Marangoni stress that could balance the electro-osmotic stress (Baygents & Saville 1991). Thus, experimental studies of the electrokinetic mobilities in liquid/liquid systems will be sensitive to contaminants present at the interface, and experimental systems should be chosen with care.

Finally, experimental realization of electrokinetics with moderately conductive liquids may utilize an 'interface between two immiscible electrolytic solutions' system (ITIES) (Girault & Schiffrin 1989). ITIES posess many of the properties that are required for an electrokinetics study: they are well-characterized in the electrochemistry literature, the phases are immiscible, the interface is ideally polarizable over a range of potentials, and the conductivity (and Debye length) of each phase can be adjusted independently (Girault & Schiffrin 1989; Daikhin & Urbakh 2003; Monroe, Urbakh & Kornyshev 2009).

We gratefully acknowledge support from the NSF CAREER program (CBET-645097) and the Arnold and Mabel Beckman Foundation.

REFERENCES

AUDRY, M., PIEDNOIR, A., JOSEPH, P. & CHARLAIX, E. 2010 Amplification of electro-osmotic flows by wall slippage: direct measurements on OTS-surfaces. *Faraday Discuss.* **146**, 113–124.

BAGOTSKAYA, I. A. 1949 Dvizhenie zhidkikh i tverdykh metallicheskikh chastits v rastvorakh elektrolitov .5. opytnaya proverka uravnenii dvizheniya kapel rtuti v elektricheskom pole. *Zh. Fiz. Khim.* **23** (10), 1231–1238.

BAHGA, S. S., VINOGRADOVA, O. I. & BAZANT, M. Z. 2010 Anisotropic electro-osmotic flow over super-hydrophobic surfaces. *J. Fluid Mech.* **644**, 245–255.

BAYGENTS, J. C. & SAVILLE, D. A. 1991 Electrophoresis of drops and bubbles. *J. Chem. Soc. Faraday Trans.* **87** (12), 1883–1898.

BAZANT, M. Z. & SQUIRES, T. M. 2010 Induced-charge electrokinetic phenomena. *Curr. Opin. Colloid Interface Sci.* **15** (3), 203–213.

BOCQUET, L. & CHARLAIX, E. 2010 Nanofluidics, from bulk to interfaces. *Chem. Soc. Rev.* **39** (3), 1073.

BOOTH, F. 1951 The cataphoresis of spherical fluid droplets in electrolytes. *J. Chem. Phys.* **19** (11), 1331–1336.

BOUZIGUES, C. I., TABELING, P. & BOCQUET, L. 2008 Nanofluidics in the debye layer at hydrophilic and hydrophobic surfaces. *Phys. Rev. Lett.* **101** (11), 114503–4.

CHU, K. T. & BAZANT, M. Z. 2007 Surface conservation laws at microscopically diffuse interfaces. *J. Colloid Interface Sci.* **315** (1), 319–329.

CHURAEV, N. V., RALSTON, J., SERGEEVA, I. P. & SOBOLEV, V. D. 2002 Electrokinetic properties of methylated quartz capillaries. *Adv. Colloid Interface Sci.* **96** (1–3), 265–278.

https://doi.org/10.1017/jfm.2011.288 Published online by Cambridge University Press

DAIGUJI, H., OKA, Y. & SHIRONO, K. 2005 Nanofluidic diode and bipolar transistor. *Nano Lett.* **5** (11), 2274–2280.

DAIKHIN, L. I. & URBAKH, M. 2003 Double layer capacitance and a microscopic structure of electrified liquid–liquid interfaces. *J. Electroanalyt. Chem.* **560** (1), 59–67.

DAVIDSON, C. & XUAN, X. 2008 Electrokinetic energy conversion in slip nanochannels. *J. Power Sources* **179** (1), 297–300.

DORFMAN, K. D. 2010 DNA electrophoresis in microfabricated devices. *Rev. Mod. Phys.* **82** (4), 2903.

DUKHIN, S. S. 1993 Nonequilibrium electric surface phenomena. *Adv. Colloid Interface Sci.* **44**, 1–134.

FRUMKIN, A. 1946 New electrocapillary phenomena. *J. Colloid Sci.* **1** (3), 277–291.

GAMAYUNOV, N. I., MANTROV, G. I. & MURTSOVKIN, V. A. 1992 Study of flows induced in the vicinity of conducting particles by an external electric-field. *Colloid J. USSR* **54** (1), 20–23.

GIRAULT, H. & SCHIFFRIN, D. 1989 Electrochemistry of liquid–liquid interfaces. In *Electroanalytical Chemistry,* vol. 15. Marcel-Dekker.

GÖRG, A., WEISS, W. & DUNN, M. J. 2004 Current two-dimensional electrophoresis technology for proteomics. *Proteomics* **4** (12), 3665–3685.

GORRE, L., IOANNIDIS, E. & SILBERZAN, P. 1996 Rectified motion of a mercury drop in an asymmetric structure. *Europhys. Lett.* **33** (4), 267–272.

GORRE-TALINI, L. & SILBERZAN, P. 1997 Force-free motion of a mercury drop alternatively submitted to shifted asymmetric potentials. *J. Phys.* I **7** (11), 1475–1485.

HENRY, D. C. 1931 The cataphoresis of suspended particles. Part 1. The equation of cataphoresis. *Proc. R. Soc. Lond.* A **133** (821), 106–129.

JOLY, L., YBERT, C., TRIZAC, E. & BOCQUET, L. 2006 Liquid friction on charged surfaces: from hydrodynamic slippage to electrokinetics. *J. Chem. Phys.* **125** (20).

KARNIK, R., DUAN, C., CASTELINO, K., DAIGUJI, H. & MAJUMDAR, A. 2007 Rectification of ionic current in a nanofluidic diode. *Nano Lett.* **7** (3), 547–551.

KHAIR, A. S. & SQUIRES, T. M. 2008*a* Fundamental aspects of concentration polarization arising from nonuniform electrokinetic transport. *Phys. Fluids* **20** (8), 087102–20.

KHAIR, A. S. & SQUIRES, T. M. 2008*b* Surprising consequences of ion conservation in electro-osmosis over a surface charge discontinuity. *J. Fluid Mech.* **615**, 323–334.

KHAIR, A. S. & SQUIRES, T. M. 2009*a* The influence of hydrodynamic slip on the electrophoretic mobility of a spherical colloidal particle. *Phys. Fluids* **21** (4), 042001–14.

KHAIR, A. S. & SQUIRES, T. M. 2009*b* Ion steric effects on electrophoresis of a colloidal particle. *J. Fluid Mech.* **640**, 343–356.

KIM, S. J., KO, S. H., KANG, K. H. & HAN, J. 2010 Direct seawater desalination by ion concentration polarization. *Nat. Nano.* **5** (4), 297–301.

LANDERS, J. P. 2003 Molecular diagnostics on electrophoretic microchips. *Analyt. Chem.* **75** (12), 2919–2927.

LARSEN, R. J., DICKEY, M. D., WHITESIDES, G. M. & WEITZ, D. A. 2009 Viscoelastic properties of oxide-coated liquid metals. *J. Rheol.* **53** (6), 1305–1326.

LAUGA, E., BRENNER, M. & STONE, H. 2007 Microfluidics: the no-slip boundary condition. In *Handbook of Experimental Fluid Mechanics*, pp. 1219–1240. Springer.

LEINWEBER, F. C., EIJKEL, J. C. T., BOMER, J. G. & VAN DEN BERG, A. 2006 Continuous flow microfluidic demixing of electrolytes by induced charge electrokinetics in structured electrode arrays. *Analyt. Chem.* **78** (5), 1425–1434.

LEINWEBER, F. C. & TALLAREK, U. 2005 Concentration polarization-based nonlinear electrokinetics in porous media: induced-charge electroosmosis. *J. Phys. Chem.* B **109** (46), 21481–21485.

LEVICH, V. G. 1962 *Physicochemical Hydrodynamics*. Prentice-Hall.

LEVINE, S. & O'BRIEN, R. N. 1973 Theory of electrophoresis of charged mercury drops in aqueous-electrolyte solution. *J. Colloid Interface Sci.* **43** (3), 616–629.

LÓPEZ-GARCÍA, J., ARANDA-RASCÓN, M. & HORNO, J. 2008 Excluded volume effect on the electrophoretic mobility of colloidal particles. *J. Colloid Interface Sci.* **323** (1), 146–152.

LYKLEMA, J. 1995 *Fundamentals of Interface and Colloid Science,* vol. 2. Academic.

LYKLEMA, J. 2003 Electrokinetics after smoluchowski. *Colloid Surf.* A **222** (1–3), 5–14.

https://doi.org/10.1017/jfm.2011.288 Published online by Cambridge University Press

MANI, A., ZANGLE, T. A. & SANTIAGO, J. G. 2009 On the propagation of concentration polarization from microchannel–nanochannel interfaces part i: analytical model and characteristic analysis. *Langmuir* **25** (6), 3898–3908.

MANSURIPUR, T. S., PASCALL, A. J. & SQUIRES, T. M. 2009 Asymmetric flows over symmetric surfaces: capacitive coupling in induced-charge electro-osmosis. *New J. Phys.* **11** (7), 075030.

MESSINGER, R. J. & SQUIRES, T. M. 2010 Suppression of electro-osmotic flow by surface roughness. *Phys. Rev. Lett.* **105** (14), 144503.

MONROE, C. W., URBAKH, M. & KORNYSHEV, A. A. 2009 Double-layer effects in electrowetting with two conductive liquids. *J. Electrochem. Soc.* **156** (1), P21.

MULLER, V., SERGEEVA, I., SOBOLEV, V. & CHURAEV, N. 1986 Boundary effects in the theory of electrokinetic phenomena. *Colloid J. USSR* **48** (4), 606–614.

MURTSOVKIN, V. A. 1996 Nonlinear flows near polarized disperse particles. *Colloid J. USSR* **58** (3), 341–349.

O'BRIEN, R. W. 1983 The solution of the electrokinetic equations for colloidal particles with thin double layers. *J. Colloid Interface Sci.* **92** (1), 204–216.

O'BRIEN, R. W. & WHITE, L. R. 1978 Electrophoretic mobility of a spherical colloidal particle. *J. Chem. Soc. Faraday Trans.* 2 **74**, 1607–1626.

OHSHIMA, H. 1997 A simple expression for the electrophoretic mobility of charged mercury drops. *J. Colloid Interface Sci.* **189** (2), 376–378.

OHSHIMA, H., HEALY, T. W. & WHITE, L. R. 1984 Electrokinetic phenomena in a dilute suspension of charged mercury drops. *J. Chem. Soc. Faraday Trans.* 2 **80** (12), 1643–1667.

PASCALL, A. J. & SQUIRES, T. M. 2010*a* An automated, high-throughput experimental system for induced charge electrokinetics. *Lab on a Chip* **10** (18), 2350–2357.

PASCALL, A. J. & SQUIRES, T. M. 2010*b* Induced charge electro-osmosis over controllably contaminated electrodes. *Phys. Rev. Lett.* **104** (8), 088301.

PENNATHUR, S., EIJKEL, J. C. T. & VAN DEN BERG, A. 2007 Energy conversion in microsystems: is there a role for micro/nanofluidics? *Lab on a Chip* **7** (10), 1234.

POIGIN, B. N., PANFILOV, A. M., NEMCHENKO, V. P. & POPEL, S. I. 1977 Electrocapillary motion of mercury drops in strong electric-fields. *Sov. Electrochem.* **13** (3), 294–297.

REN, Y. & STEIN, D. 2008 Slip-enhanced electrokinetic energy conversion in nanofluidic channels. *Nanotechnology* **19** (19), 195707.

RUSSEL, W. B., SAVILLE, D. A. & SCHOWALTER, W. R. 1989 *Colloidal Dispersions*. Cambridge University Press.

SCHOCH, R. B., HAN, J. & RENAUD, P. 2008 Transport phenomena in nanofluidics. *Rev. Mod. Phys.* **80** (3), 839–883.

SO, J. & DICKEY, M. D. 2011 Inherently aligned microfluidic electrodes composed of liquid metal. *Lab on a Chip* **11** (5), 905.

SQUIRES, T. M. 2008 Electrokinetic flows over inhomogeneously slipping surfaces. *Phys. Fluids* **20** (9), 092105.

SQUIRES, T. M. & BAZANT, M. Z. 2004 Induced-charge electro-osmosis. *J. Fluid Mech.* **509**, 217–252.

SQUIRES, T. M. & QUAKE, S. R. 2005 Microfluidics: fluid physics at the nanoliter scale. *Rev. Mod. Phys.* **77** (3), 977–1026.

TANDON, V. & KIRBY, B. J. 2008 Zeta potential and electroosmotic mobility in microfluidic devices fabricated from hydrophobic polymers: 2. Slip and interfacial water structure. *Electrophoresis* **29** (5), 1102–1114.

VELEV, O. D. & BHATT, K. H. 2006 On-chip micromanipulation and assembly of colloidal particles by electric fields. *Soft Matt.* **2** (9), 738.

VLASSIOUK, I., SMIRNOV, S. & SIWY, Z. 2008 Ionic selectivity of single nanochannels. *Nano Lett.* **8** (7), 1978–1985.

WANG, Y., STEVENS, A. L. & HAN, J. 2005 Million-fold preconcentration of proteins and peptides by nanofluidic filter. *Analyt. Chem.* **77** (14), 4293–4299.

ZANGLE, T. A., MANI, A. & SANTIAGO, J. G. 2009 On the propagation of concentration polarization from microchannel–nanochannel interfaces part II: numerical and experimental study. *Langmuir* **25** (6), 3909–3916.

ZHAO, H. 2010 Electro-osmotic flow over a charged superhydrophobic surface. *Phys. Rev.* E **81** (6), 066314.

https://doi.org/10.1017/jfm.2011.288 Published online by Cambridge University Press